J Mater Sci: Mater Med (2008) 19:2743–2749
DOI 10.1007/s10856-008-3401-x

Zirconia toughened alumina ceramic foams for potential bone graft applications: fabrication, bioactivation, and cellular responses

X. He · Y. Z. Zhang · J. P. Mansell · B. Su

Received: 11 October 2007 / Accepted: 5 February 2008 / Published online: 29 February 2008

Abstract Zirconia toughened alumina (ZTA) has been regarded as the next generation orthopedic graft material due to its excellent mechanical properties and biocompatibility. Porous ZTA ceramics with good interconnectivity can potentially be used as bone grafts for load-bearing applications. In this work, three-dimensional (3D) interconnected porous ZTA ceramics were fabricated using a direct foaming method with egg white protein as binder and foaming agent. The results showed that the porous ZTA ceramics possessed a bimodal pore size distribution. Their mechanical properties were comparable to those of cancellous bone. Due to the bio-inertness of alumina and zirconia ceramics, surface bioactivation of the ZTA foams was carried out in order to improve their bioactivity. A simple NaOH soaking method was employed to change the surface chemistry of ZTA through hydroxylation. Treated samples were tested by conducting osteoblast-like cell culture in vitro. Improvement on cells response was observed and the strength of porous ZTA has not been deteriorated after the NaOH treatment. The porous 'bio-activated' ZTA ceramics produced here could be potentially used as non-degradable bone grafts for load-bearing applications.

1 Introduction

Nowadays, the increasing number of bone-grafting procedures has created a shortage in the availability of musculoskeletal donor bone tissue. Developing artificial bone graft ceramic materials is therefore becoming a promising approach for the repair of large segmental bone defects [1]. In this regard, ceramic materials such as hydroxyapatite (HA), tricalcium phosphate, bioglasses, alumina and zirconia are of particular interest and have been widely investigated due to their biocompatibility and/or osteoconductivity. Among them, the calcium phosphate materials of HA and tricalcium phosphate, despite their attractive bioactivity, are notorious for their poor mechanical performance, which makes them merely suitable for uses of filling small bone defects [2] or coating other bio-inert materials [3]. It has been known that alumina in its dense form is by far the most widely used ceramic in the total hip arthroplasty because of its excellent mechanical properties and wear resistance [4]. However, they are regarded as bio-inert materials. Although porous alumina has been investigated for bone graft applications, [5] the strength decrease resulted from porous structure calls for developing ultra-strong and toughened materials for load-bearing applications. In this context, zirconia toughened alumina (ZTA) could be a candidate material for load-bearing applications due to its higher strength and fracture resistance compared to pure alumina. So far investigations carried out for the ZTA ceramics have been based on the dense form mostly for orthopedic applications [6]. To the best of our knowledge, no porous ZTA has been studied as a candidate for such applications as bone graft.

In this work, the fabrication and characterization of porous ZTA ceramics for potential load-bearing bone graft application was investigated. An interconnected 3D porous structure was produced through a direct foaming method using environmentally friendly egg white protein, which overcame the inevitable holes or carbonaceous residue at the centre of each strut during the pyrolysis of traditional

X. He (✉) · Y. Z. Zhang · J. P. Mansell · B. Su
Department of Oral and Dental Science, University of Bristol, Lower Maudlin Street, Bristol BS1 2LY, UK
e-mail: xing.he@bris.ac.uk

polymer sponge replica method [7]. Protein foaming method also avoided toxic gel-casting alternatives for the fabrication of porous ceramics. The compressive strength was tested to compare with natural human bone. Furthermore, because of the bio-inertness of ZTA, a simple bioactivation process by NaOH treatment was used to improve their surface bioactivity. Their cellular responses and possible bioactivation mechanisms were discussed.

2 Experimental

2.1 Materials

Alumina (Alcoa CT 3000 SG, USA) and Zirconia powder (Tosoh TZ-3YS-E, Japan) were used as the basic ceramic powders for the fabrication of ZTA foams. Zirconia powder has a surface area of 16 ± 3 m^2/g and a density of 6.05 g/cm^3, whereas alumina powder has a surface area of 7 m^2/g and a density of 3.96 g/cm^3. An ammonium polyacrylate (MW = 6,000) solution (Darvan 821A, R. T. Vanderbilt Inc., USA) was used as electrosteric dispersant. Egg-white protein (albumin, Danish pasteurized spray dried, Lactosan-Sanovo (UK) Limited) was employed as a binder and foaming agent. Distilled water was used as a solvent.

2.2 Fabrication of porous ceramics

Porous ZTA composite foams were produced from a direct foaming method using egg white protein as a binder and foaming agent [8, 9] with a procedure as shown in Fig. 1. Briefly, Al_2O_3 and ZrO_2 powders at a weight ratio of 9:1 were dispersed at a volume ratio of 40% in distilled water using dispersant Darvan 821A. Thus formed slurry in a water-proof polypropylene bottle was ball milled for 24 h. Then the egg white protein powder was added in and mixed for another hour. Afterwards the bottle was set upside-down milling for agitation to induce air bubbles forming. Generally uniform air bubbles could be achieved in 20 h. Then the slurry was poured into rectangular moulds, which were pre-dried in an oven at 40 °C overnight. Finally the cast green body was sintered at 1650 °C for 2 h. Such produced porous ZTA ceramics were cut into small cubic pieces for subsequent bioactivation treatment and characterization.

2.3 Characterization of the microstructure

Scanning electron microscope (Cambridge 90B Stereoscan, UK) was used to observe the pore morphology and measure the pore size distributions. The open porosity of such porous samples was measured using traditional

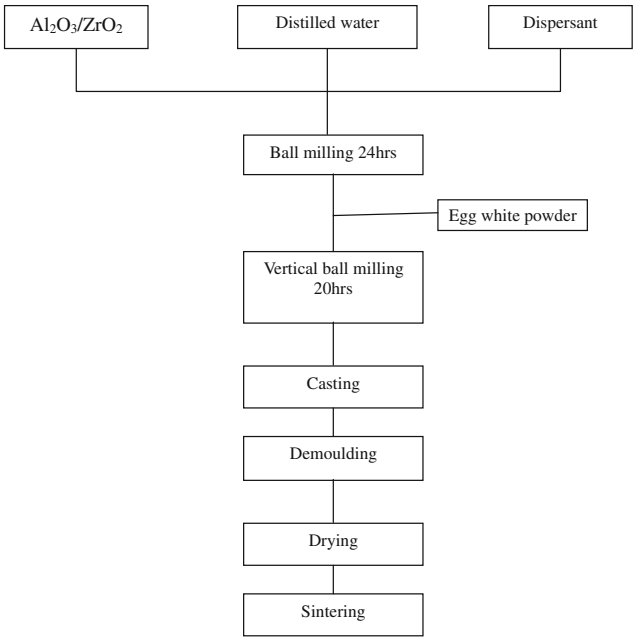

Fig. 1 A flow chart showing the procedure in fabricating porous ZTA ceramics

Archimedes method [10]. In brief, the dry sample with a mass of m_1 was boiled in water for 30 min to remove the air trapped in the pores. Then it was cooled down to ambient temperature, and weighed to have the sample weights of being infiltrated with water (m_2) and being immersed in water (m_3). The open porosity was calculated using the following equation (1).

$$\rho_{open} = \frac{m_2 - m_1}{m_2 - m_3} \times 100\% \quad (1)$$

Determination of the apparent porosity was based on the equation (2), where ρ_b is the bulk density of the porous ZTA ceramics, and ρ_s is the average density of fully dense polycrystalline zirconia (6.05 g/cm^3) and alumina (3.96 g/cm^3).

$$\rho_{app} = \left(1 - \frac{\rho_b}{\rho_s}\right) \times 100\% \quad (2)$$

2.4 Bioactivation

All porous cubic ceramic samples were aliquot divided and soaked in 5 M NaOH solution at 80 °C for 0, 5, 10, 24, and 48 h, respectively. A Fourier Transform Infrared (FTIR) analysis (Shimadzu Corp., FTIR 8300) was used to measure treated alumina/zirconia powders, which had been soaked at the same conditions as the porous ceramic samples. The spectra of alumina/zirconia powders were recorded by the data processing software (Shimadzu Corp., Hyper IR) with 8 cm^{-1} of resolution and 100 scanning times. The samples and background spectra were collected

in power mode and stored as single beam spectra for further processing. Prior to the FTIR scanning, the ceramic powders were washed several times to eliminate residual NaOH. To increase the spectrum signal from the powders and to avoid influences of water absorbed on KBr, the washed powders were placed in a micro sample holder and dried overnight at 110 °C.

2.5 Mechanical testing

Samples with a dimension of $10 \times 10 \times 5$ mm^3 were cut with an Accutom-5 (Struers, UK) cutting machine for compressive tests using a uni-axial mechanical tester (Lloyd Instruments LR5K, UK). The crosshead speed used is 0.5 mm/s. Compressive strength was derived from the test curves. Furthermore, strength data were analyzed using Weibull statistics, with a maximum likelihood approach to estimating the characteristic strength and Weibull modulus. 10 samples of each soaking treatment condition were tested.

2.6 In vitro cell culture

To evaluate cellular responses to the developed porous ZTA ceramics, untreated and treated materials were tested with human osteoblasts-like cells (MG63) cultured in vitro. The MG63 cells were grown to confluence in DMEM/F12 nutrient mix, then dispensed into 24-well plates (Greiner, Frickenhausen, Germany) such that each well contained 1 mL of a 2.0×10^4 cells suspension (as assessed by haemocytometry). Cells were then cultured for 65 h, the media were removed and the cells were treated with the same medium but lacking serum for 24 h to synchronize the cells. After the 24 h starve period, medium was removed and cells treated with media containing a combination of vitamin D3 with serum. Then all experiments were left for 72 h prior to an assessment of cell number and alkaline phosphatase activity as per previously used protocols [11].

For SEM imaging of the cell morphology on the ZTA samples, cell fixation was performed as follows. The samples were first treated with 2.5% glutaraldehyde in PBS for one hour in room temperature. They were then dehydrated successively for 30 min each in 20%, 40%, 60%, 80% and 100% analytical grade ethanol and finally in hexamethyldisilazane. The samples with fixed cells were coated with Pt/Pd prior to SEM imaging. Cell culture samples were fixed for imaging after 72 h of cell culture.

3 Results and discussion

3.1 Morphology of the porous ZTA

Typical morphology of the direct formed porous ZTA ceramics was shown in Fig. 2a. It can be seen that the large pores were in spherical shape and interconnected by small windows/holes in the spherical pore walls. The spherical pore walls and struts were dense, and no macroscopic cracks or defects were observed after sintering. A close-up view of the sintered ZTA ceramic showed a very uniform dispersion of zirconia grains within the alumina grains matrix (Fig. 2b). The zirconia grains with sizes of several times finer than the alumina grains size were situated at intergranular positions, such as grain boundaries and triple points. This will improve the micro-cracking resistance and result in improved fracture toughness of brittle alumina [6, 12].

The mechanism of forming current spherical shaped pores and the windows presented in the spherical pore walls are explained as follows. First of all, those spherical-shaped pores are originated from the inherent foaming ability of a liquid. After ceramic particles were well dispersed in water, the egg white protein was added to facilitate the formation of liquid foams during agitation by ball milling. Thermodynamically unstable liquid foams may collapse within a few seconds due to their high gas–liquid interfacial tension [13]. Whereas long-chain

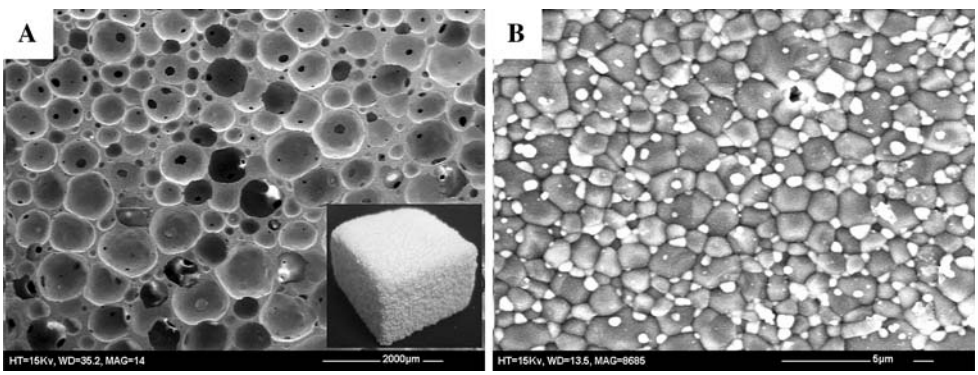

Fig. 2 SEM microphotographs of porous ZTA ceramics. (**a**) A general view (inset photograph shows the actual 3-D porous ZTA ceramic), and (**b**) a close-up view of the ZTA ceramic, with the brighter and darker grains representing the phases of zirconia and alumina, respectively

polymers, like egg white protein, can prolong the foam lifetime from a few minutes to several hours by adsorbing at the air-water interface. On the other hand, ceramic particles adsorbed on the air-liquid interfaces of ceramic particle/egg white protein can dramatically decrease overall system free energy and synergistically stabilize and prolong the sustainable time. But because of the difference of capillary pressure at the junctions of struts in liquid foams and in the foam membranes; this resulted in greater curvature of the liquid-gas interfaces in the foam membranes. Thus, the ceramic slurry was prone to flow from the membranes to the struts, leading to thinning of spherical pore walls; eventually rupturing to form small windows in the spherical pore walls (Fig. 2a) and fully dense ceramic struts after sintering [14].

The apparent and open porosities of current direct foamed porous ZTA ceramic samples were found to be 79% and 77%, respectively, indicating good pore interconnectivity. It has been known that a porous structure with a porosity above 60% generally resulted in increasing possibility of pore interconnection due to the packing density of randomly distributed spherical pores [15]. Figure 3 shows the pore size distribution based on the measurements on the SEM images of the porous ZTA ceramic. The two distinctive pore ranges of 0–300 μm (small) and 300–1,000 μm (large) suggest that the pore size distribution is bimodal. Large pores are associated with those spherical shaped pores (Fig. 2a), and the small pores correspond to the interconnecting small windows (Fig. 2a) in the spherical pore walls which provide pores interconnectivity, an important consideration in terms of encouraging to form good tissue-graft integration/bonding and facilitating the nutrition and waste transportation during tissue growth.

3.2 Bioactivation

It has been widely accepted that bioactivation of ceramic bone grafts could encourage strong interfacial bonding with bone and stress-stimulated bone growth [3, 16, 17]. HA, as the natural mineral phase in bone, has been commonly used for such purposes through being coated to bioinert implants by pulsed laser deposition or plasma spray techniques [18]. However, these line-of-sight techniques could not be used to coat porous ceramic materials. Although methods such as sol-gel coating, ceramic slurry dipping, and biomimetic approach using a stimulated body fluid have been explored [3, 19]for coating porous scaffolds, the weak bond strengths between HA coating layer and base materials caused difficulties for practical applications. As such, in this study we employed a chemical treatment method [20], i.e., using NaOH solution soaking treatment for hydroxylation, to minimize the noted interfacial bonding problems and to improve bioactivity of the porous ZTA ceramics. According to Fisher et al. [20] during the NaOH solution soaking treatment, following reaction (Eq. 3) might have occurred:

$$Al_2O_3 + 2NaOH + 3H_2O \rightarrow 2Na^+ + 2[Al(OH)_4]^- \quad (3)$$

Hydroxylation was proved through our FTIR analysis. The post-treatment alumina surfaces have exhibited the hydrogen bonded water molecular or free hydroxyls groups. As shown in Fig. 4, FTIR spectra clearly showed broad peaks at 3450 cm^{-1} ascribed to hydrogen bonded surface hydroxyl modes, and small peaks at 3690 cm^{-1} assigned to free hydroxyl groups, which are in good agreement with the results reported in literature [21]. The FTIR spectra also indicate that the treatment time has less significant influence on the extent of hydroxylation.

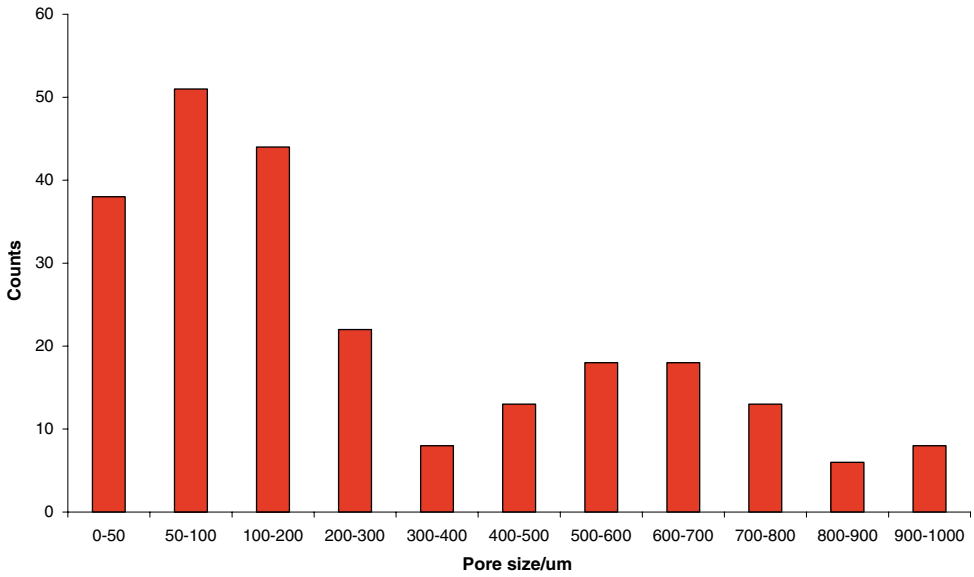

Fig. 3 Pore size distribution of the directly formed porous ZTA ceramics

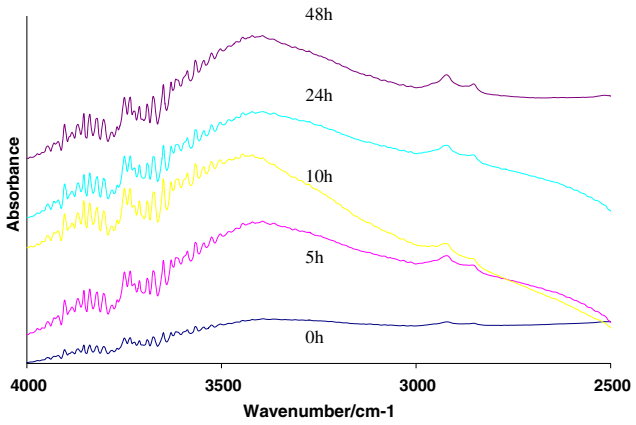

Fig. 4 FTIR spectra recorded at room temperature under dry air atmosphere of the alumina/zirconia powders treated for 0, 5, 10, 24, and 48 h

3.3 Mechanical properties

The average compressive strengths of current ZTA ceramic samples with an open porosity of 77% and treated for 0 (control), 10, and 48 h were found to be 20, 23, and 27 MPa, respectively, which show enhanced mechanical properties because of the zirconia incorporation when compared to pure alumina (ca. 15 MPa) in our previous study [22]. The compressive strength achieved is comparable to that of human cancellous bone [23]. Thus, grafts made of current porous ZTA composite materials could potentially be used in load-bearing situations. In this study we also used the Weibull modulus (M) to illustrate the compressive behavior of our porous ZTA ceramic [24]. In Fig. 5, p stands for possibility of failure and s for compressive strength (MPa). The slope of each curve gives the Weibull modulus, which is a reliability indicator for a given volume under a given stress. The Weibull moduli for samples of 0 h (control), 10 h and 48 h treatments are found to be around 3.2, suggesting a typical large scattering of strength data of the current porous ZTA ceramics. The similar Weibull moduli also imply that the harsh treatment (5 M NaOH at 80 °C) did not seem to deteriorate the compressive strength of porous ZTA composite materials. This may be explained as that the NaOH treatment may have only affected the superficial rough surfaces.

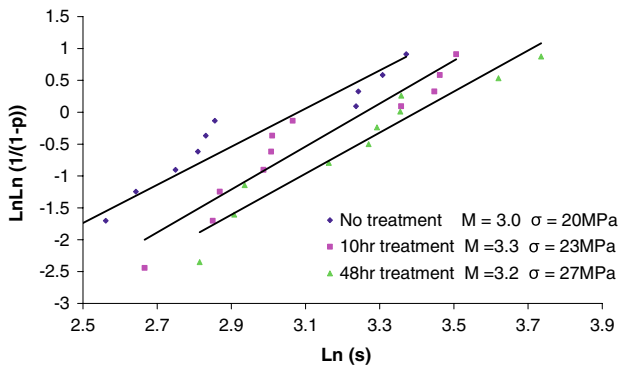

Fig. 5 Weibull plot for the compressive strength of porous ZTA samples treated with different times in 80 °C NaOH solutions

3.4 Cellular responses

Relative cellularity is a parameter to indicate the degree of cell attachment on ceramic scaffolds, which is assessed by the relative cell number per unit volume of the porous ceramics. The relative cellularity results showed in Fig. 6 indicates that soaking treatment with a period of 5–10 h of time in 80 °C NaOH solutions seemed to favor the cell adhesion and proliferation with current ZTA porous ceramics. This might be ascribed to the hydroxylation effect of ZTA surfaces because surface hydroxyl groups have been proven to promote the cell attachment [25]. One of the hypotheses was that protein adsorption was governed by alterations in hydroxyl groups of the material surface and the protein [20]. The results of alkaline phosphatase (ALP) activity shown in Fig. 7 were influenced by the treatment time of the ZTA ceramics in the similar way as

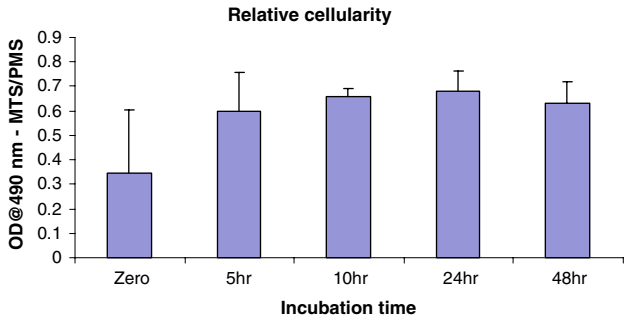

Fig. 6 Relative cellularity of the different porous ZTA ceramics (with standard deviation), which had been treated for different time in 80 °C NaOH solution

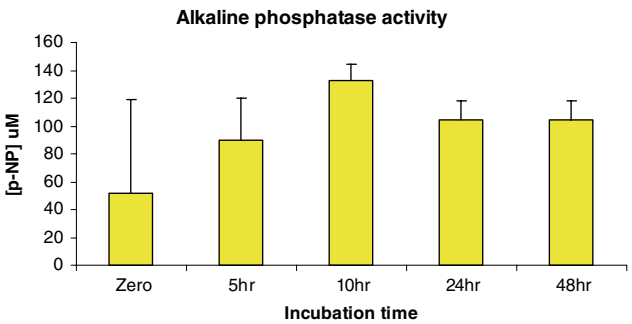

Fig. 7 ALP activity of the different porous ZTA ceramics (with standard deviation), which had been treated for different time in 80 °C NaOH solution

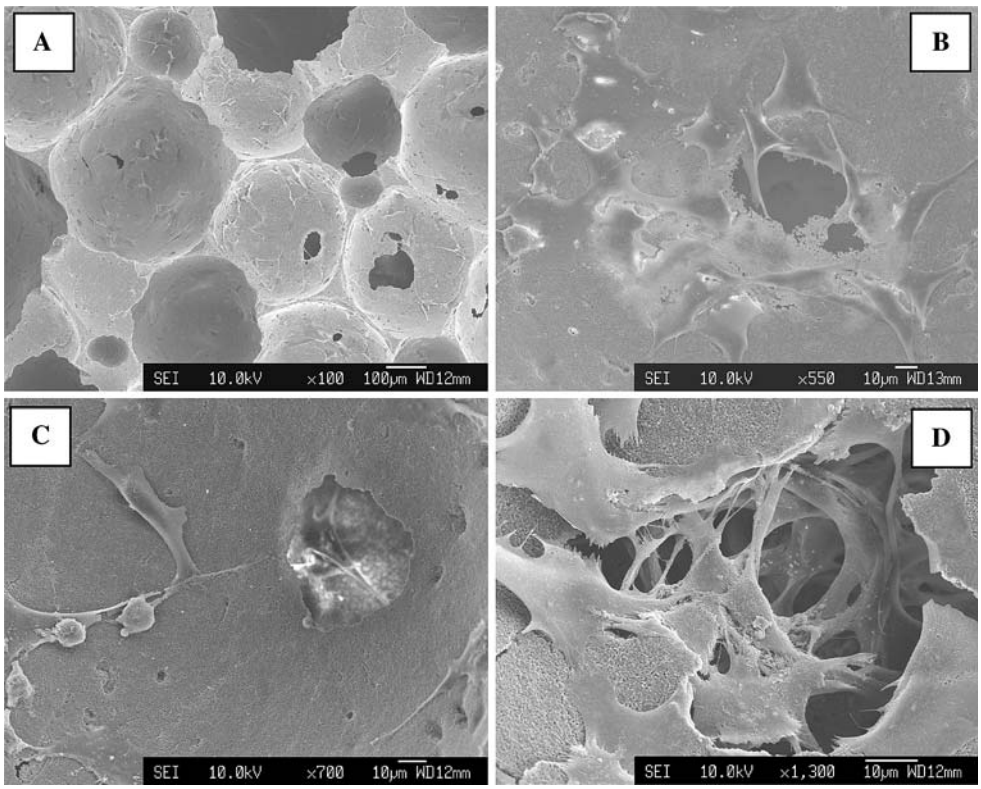

Fig. 8 Cell morphologies on/in the porous ZTA ceramics after 72 h cell culture. (**a**) An overview; (**b**) cells aggregated around the window pore; (**c**) cells inside the pore cavity; and (**d**) multilayer cells in the pore cavity

the relative cellularity. ALP was an enzyme bound to the cell membrane and could be used as a marker of osteoinductive cells. ALP is considered to play an important role in bone generation. From Figs. 6 and 7, it was also noted that large variation presented in the untreated samples. This could be due to inherent non-bioactivity attribute of the porous ZTA ceramics. Even so, it is obvious that the surface treatment had greatly improved consistence of the cell response. There seemed a clear correlation between stabilizing cell proliferation with surface hydroxylation. Further understanding of the mechanisms as well as the control of this interaction in future could lead to the optimization of the current ceramic biomaterials in bone grafts applications.

The cell morphology after culturing MG63 cells for 72 h with the porous ZTA ceramics was observed with SEM (Fig. 8). Due to the porous characteristic of ZTA, in this study there seemed difficult to visually distinguish the cell proliferation differences between the treated and untreated ZTA samples. However, localized cell morphological differences with current porous ZTA samples are still noticeable. In general, cells attached on the spherical pore walls (Fig. 8a, b) and within the pore cavities (Fig. 8c, d) were observed. There were few cells and even less lamellipodia stretched on the spherical walls than nearby or inside opening pores (Fig. 8a, c). The cells spread better and have more contact with each other nearby or inside opening pores (Fig. 8b, d). The more complex cell matrix has been found inside the pores on the treated samples (Fig. 8d). This might be because the pore opening and cavities acting as the channels for nutrition supply and waste transfer, which means more chances for cell ingrowth.

4 Conclusions

The 3D porous ZTA ceramics have been fabricated using a direct foaming method. The ZTA foams exhibited a bimodal pore distribution. The NaOH soaking treatments have resulted in the surface hydroxylation and consequently improved surface bioactivity of the porous ZTA ceramics. This seemed to have led to improved osteoblast cell attachment and differentiation. The compressive strengths of as-fabricated and surface-treated ZTA ceramics were comparable to that of the cancellous bone. The average achieved compressive strength of 20–27 MPa with a porosity of 77% could potentially meet the mechanical requirement for load-bearing applications. Further optimization in microstructure and mechanical properties is needed to warrant their application as bone grafts.

Acknowledgements Dr. RP Shellis was thanked for his help to use FTIR instrument and useful discussions. Dr. S Dhara was thanked for initial discussion.

References

1. L.L. Hench, Bioceramics. J. Am. Ceram. Soc. **81**(7), 1705–1728 (1998)
2. E. Fidancevska, G. Ruseska, J. Bossert, Y. Lin, A.R. Boccaccini, Fabrication and characterization of porous bioceramic composites based on hydroxyapatite and titania. Mater. Chem. Phys. **103**, 95–100 (2007)
3. X. Miao, Y. Hu, J. Liu, X. Huang, Hydroxyapatite coating on porous zirconia. Mater. Sci. Eng. C **27**, 257–261 (2007)
4. G. Willmann, Ceramic femoral head for total hip arthroplasty. Adv. Eng. Mater. **2**(3), 114–121 (2000)
5. S. Bose, J. Darsell, M. Kintner, H. Hosick, A. Bandyopadhyay, Pore size and pore volume effects on alumina and TCP ceramic scaffolds. Mater. Sci. Eng. C **23**, 479–486 (2003)
6. J. Pierri, E.B. Roslindo, R. Tomasi, E. Pallone, E. Rigo, Alumina/zirconia composite coated by biomimetic method. J. Non-Cryst. Solids **352**, 5279–5283 (2006)
7. F.F. Lange, K.T. Miller, Open cell, low-density ceramics fabricated from reticulated polymer substrates. Adv. Ceram. Mater. **2**(4), 827 (1987)
8. C. Tuck, J.R.G. Evans, Porous ceramics prepared from protein foams. J.Mater. Sci. Lett. **18**, 1003 (1999)
9. S. Dhara, P. Bhargava, Simple direct casting route to ceramic foams. J. Am. Ceram. Soc. **86**(10), 1645–1650 (2003)
10. A.O. Engin, A.C. Tas, Manufacture of macroporous calcium hydroxyapatite bioceramics. J. Eur. Ceram. Soc. **19**, 2569 (1999)
11. S.J. Yarram, C. Tasman, J. Gidley, M.J.R. Clare Sandy, J.P. Mansell, Epidermal growth factor and calcitriol synergistically induce osteoblast maturation. Mol Cell Endocrinol. **220**, 9–20 (2004)
12. S. Deville, J. Chevalier, G. Fantozzi et al., Low-temperature ageing of zirconia-toughened alumina ceramics and its implication in biomedical implants. J. Eur. Ceram. Soc. **23**, 2975–2982 (2003)
13. A.R. Studart, U.T. Gonzenbach, E. Tervoort et al., Processing routes to macroporous ceramics: a review. J. Am. Ceram. Soc. **89**(6), 1771–1789 (2006)
14. H.X. Peng, Z. Fan, J.R.G. Evans et al., Microstructure of ceramic foams. J. Eur. Ceram. Soc. **20**, 807–813 (2000)
15. K.A. Hing, Bioceramic bone graft substitutes: influence of porosity and chemistry. Int. J. Appl. Ceram. Technol. **2**(3), 184–199 (2005)
16. H.F. Hildebrand, N. Blanchemain, G. Mayer, F. Chai, M. Lefebvre, F. Boschin, Surface coatings for biological activation and functionalization of medical devices. Surf. Coat. Technol. **200**, 6318 (2006)
17. K. Yamashita, E. Yonehara, X.F. Ding, M. Nagai, T. Umegaki, M. Matsuda, Electrophoretic coating of multilayered apatite composite on alumina ceramics. J. Biomed. Mater. Res. **43**(1), 46–53 (1998)
18. C.F. Koch, S. Johnson, D. Kumar, M. Jelinek, D.B. Chrisey, A. Doraiswamy, C. Jin, R.J. Narayan, I.N. Mihailescu, Pulsed laser deposition of hydroxyapatite thin films. Mater. Sci. Eng. C **27**, 484–494 (2007)
19. K. Rezwana, Q.Z. Chena, J.J. Blakera, A.R. Boccaccini, Biodegradable and bioactive porous polymer/inorganic composite scaffolds for bone tissue engineering. Biomaterials **27**, 3413 (2006)
20. H. Fischer, C. Niedhart, N. Kaltenborn, A. Prange, R. Marx, F.U. Niethard, R. Telle, Bioactivation of inert alumina ceramics by hydroxylation. Biomaterials **26**, 6151–6157 (2005)
21. T. Shirai, C. Ishizaki, K. Ishizaki, Effects of Manufacturing Processes on Hydration Ability of High Purity (-Al2O3 Powders. J. Jpn. Ceram. Soc. **114**, 286–289 (2006)
22. B. Su, X. He, S. Dhara, J.P. Mansell, Porous and Bioactive Alumina Ceramics for Bone Grafts and Tissue Engineering Scaffolds. Key Eng. Mater. **330–332**, 975–978 (2007)
23. L.L. Hench, J. Wilson, *An Introduction to Bioceramics* (World Scientific, London, U.K., 1993)
24. P. Colombo, J.R. Hellmann, D.L. Shelleman, Mechanical properties of silicon oxycarbide ceramic foams. J. Am. Ceram. Soc. **84**(10), 2245 (2001)
25. K. Anselme, Osteoblast adhesion on biomaterials. Biomaterials **21**, 667 (2000)